Macromolecules
ARTICLE

Macromolecules **2009**, *42*, 7961–7968 **7961**
DOI: 10.1021/ma901298h

Explicit Sequence of Styrene/Methyl Methacrylate Gradient Copolymers Synthesized by Forced Gradient Copolymerization with Nitroxide-Mediated Controlled Radical Polymerization

Lin Wang and Linda J. Broadbelt*

Department of Chemical and Biological Engineering, Northwestern University, Evanston, Illinois 60208

Received June 16, 2009; Revised Manuscript Received August 19, 2009

ABSTRACT: In spite of many efforts made to study gradient copolymers, the monomer-by-monomer sequence along the chain is still obscure. A general computational framework based on kinetic Monte Carlo simulations was developed to predict the explicit sequence of copolymers. We demonstrate our approach using styrene (S)/methyl methacrylate (MMA) gradient copolymers synthesized by a semibatch process with nitroxide-mediated controlled radical polymerization (NM-CRP). It was found that the variation in the average segment length as a function of chain length does not resemble that of the instantaneous composition. Our findings indicate that copolymers with compositional gradients may have monomer-by-monomer sequences resembling those of statistical copolymers. It was also found that the explicit sequence can significantly deviate from that of the instantaneous composition as a function of chain length when combination is the favored termination mode. These details of explicit sequence revealed by KMC simulations are obscured by only considering fractional composition measures to characterize the gradient shape.

Introduction

Gradient copolymers are a relatively new type of copolymer, which are expected to have an intermediate chain architecture between conventional block copolymers and random copolymers.[1] As shown in Scheme 1, the most identifiable and appealing feature of this chain sequence is that segments comprising the chain vary in length according to a certain pattern from one end to the other.[2] Because of the well-ordered variation in chain structure, gradient copolymers have been theorized to exhibit interfacial activities superior to block copolymers of the same composition.[3−8] Gradient copolymers have been used in a wide range of applications ranging from compatibilizers for polymer blends to functional nanostructured materials.

The majority of gradient copolymers reported so far are synthesized using living radical polymerization (LRP) in which the lifetime of most propagating radicals is equal to as long as the total reaction time because of a reversible activation/deactivation procedure.[9] Because of this unique feature of LRP, the monomer composition in the reaction mixture can be changed during the growth of a copolymer chain, which makes it possible to predesign the monomer-by-monomer sequence along the chain and thus form the well-defined sequence of gradient copolymers depicted in Scheme 1. The monomer composition is normally varied by compositional drift or the addition of the second monomer during the reaction.[10] It has been reported recently that several new synthesis approaches other than LRP can also be used to make gradient copolymers, such as conformation-dependent sequence design (CDSD).[11]

Gradient copolymers have been reported to have microphase separation like block copolymers, and the interface region between the chemically different regions is theorized to be more blurred than conventional block copolymers of the same composition due to the variation in the block lengths along the gradient copolymer chain, which may offer a large degree of control over the interfacial profile.[4,7] Experimental investigations have confirmed that the bulk and interfacial activity of copolymers depends on the comonomer sequence distribution.[7,12] Furthermore, many properties of gradient copolymers, such as glass transition temperature and lower critical solution temperature, can be also affected by their microscopic monomer-by-monomer sequences.[6,13]

However, unlike block copolymers, the monomer-by-monomer sequences in gradient copolymers cannot be determined directly by experimental methods because multiple segments are formed continuously during the reaction along the copolymer chain. The formation of a gradient sequence is currently characterized indirectly by the variation of overall composition (cumulative composition F or instantaneous composition F_{inst}) as a function of average chain length or conversion.[1,2,4,14−18] In a successful synthesis of gradient copolymers, the overall composition varies monotonically and continuously as a chain grows, which is not observed in the synthesis of random copolymers or block copolymers.

There have been efforts to simulate the variation of F_{inst} and F as a function of average chain length during the synthesis of gradient copolymers in the past decade. For example, Beginn developed a mathematical model to simulate the compositional gradient formed along the chain.[19] Zhu et al. built a continuum model to simulate the variation of F_{inst} as a function of average chain length in a semibatch process with reversible addition−fragmentation transfer radical polymerization (RAFT).[20,21]

Although the monomer-by-monomer sequence along the copolymer chain plays an important role in the research and potential applications of gradient copolymers, few efforts have been directed at the investigation of the explicit sequence of gradient copolymers. The average sequence length and sequence length distribution can be predicted using a probabilistic model describing conventional free radical polymerization (FRP).[22] For

*To whom correspondence should be addressed. E-mail: broadbelt@northwestern.edu. Phone: 847 491 5351. Fax: 847 491 3728.

Published on Web 09/02/2009

example, Khokhlov et al. have developed a probabilistic model to predict sequence in copolymers synthesized by CDSD.[11,23,24] However, these statistical models widely used to predict sequence in FRP are not applicable in LRP because of the reversible activation/deactivation procedure between radicals and capping agents.[22] Thus, it is necessary to involve all the steps of a detailed reaction mechanism in the mathematical model in order to simulate the sequence of gradient copolymer chains. Continuum approaches have been used in a limited capacity to simulate sequence information along copolymer chains synthesized by LRP. Tabash et al. utilized a digital encoding technique and continuum models to predict sequence information for extremely short polymer chains (less than six repeat units long).[25] Zargar et al. predicted the average length of the last segments formed at the end of the reaction in an LRP system.[18] However, the number of equations required in continuum simulations increases dramatically in order to predict more explicit details of sequence, which restricts the structural information that can be predicted to a limited range of details.

What exactly are the sequences of monomers along the chain in gradient copolymers? This is a question which has been raised since the introduction of gradient copolymers[2] but has not been clearly answered yet. Here, we report the development of a simulation framework based on kinetic Monte Carlo written in house, which can predict the explicit sequence formed along each chain by tracking the growth of each individual chain instead of concentration.[26] The framework is generally applicable to various reaction types and can incorporate differences in reactivity of different chain ends in a facile way. We use this framework to investigate the explicit sequence along the backbone of MMA/S gradient copolymers prepared by NM-CRP in a semibatch reactor as an example. This system serves as a good example because S/MMA copolymerization by NM-CRP has been widely studied, and detailed kinetic parameters are available in literature.[27−41]

Development of Mathematical Model

KMC Framework. The reaction occurring at a specific instant is determined stochastically based on reaction probabilities:[26]

$$\sum_{v=1}^{\mu-1} P_v < r_1 < \sum_{v=1}^{\mu} P_v \tag{1}$$

where μ is the index of the selected reaction channel, P_v is the probability of the vth reaction channel, and r_1 is a random number uniformly distributed between 0 and 1. The probability for each reaction is determined based on its fraction of the total rate of reaction:

$$P_v = \frac{R_v}{\sum_{v=1}^{M} R_v} \tag{2}$$

where R_v is the stochastic rate of the vth reaction. The time interval between reactions is determined by

$$\tau = \frac{1}{\sum_{v=1}^{M} R_v} \ln\left(\frac{1}{r_2}\right) \tag{3}$$

where r_2 is a second random number uniformly distributed between 0 and 1. The model was developed based on elementary reactions including initiation, propagation, termination, and combination/dissociation with nitroxyl radicals. The basic reaction mechanism of copolymerization via NM-CRP using a unimolecular initiator is shown in Figure 1.

Unimolecular Initiation

$$A-T \xrightarrow{k_d} A\bullet + T\bullet$$

$$A\bullet + M \xrightarrow{k_p^M} P_1\bullet$$

Propagation

$$P_x\bullet + M \xrightarrow{k_p} P_{x+1}$$

Reversible Activation/Deactivation

$$P_x\bullet + T\bullet \underset{k_{dc}}{\overset{k_c}{\longleftrightarrow}} P_x - T$$

Termination

$$P_x\bullet + P_y\bullet \xrightarrow{k_{tc}} D_{x+y}$$

$$P_x\bullet + P_y\bullet \xrightarrow{k_{td}} D_x + D_y$$

Figure 1. Mechanism of NM-CRP using BlocBuilder as a unimolecular initiator (A−T).

(a)

$$S-S*+M \rightarrow S-M*$$
$$S-M*+M \rightarrow M-M*$$
$$S-M*+S \rightarrow M-S*$$
$$M-M*+S \rightarrow M-S*$$
$$M-S*+S \rightarrow S-S*$$
$$M-S*+M \rightarrow S-M*$$

(b)

$$S-S*+SG1 \rightarrow S-S-SG1$$
$$S-M*+SG1 \rightarrow S-M-SG1$$
$$M-S*+SG1 \rightarrow M-S-SG1$$
$$M-M*+SG1 \rightarrow M-M-SG1$$

Figure 2. Switch of categories of living chains by changing (a) ultimate and penultimate units (b) living status.

Although the different reactions are not shown explicitly in Figure 1, differences in reactivity of different chain ends, including penultimate effects on propagation reactions between propagating radicals and monomers as well as decoupling reactions of dormant chains, were incorporated. This is particularly relevant for the MMA/S system studied here. NM-CRP provides a poor degree of control over the polymerization of methacrylic esters. The dissociation rate constant k_d of MMA-terminated chains coupled with a nitroxide is too high to maintain the concentration of free radicals sufficiently low to suppress termination reactions, and the activation energy E_a of the dissociation rate constants of the dormant chains can be dramatically affected by the penultimate unit.[27] In order to capture all these kinetic details in the simulations, we subdivided radical chains and dormant chains according to their ultimate and penultimate units: M−M*, M−S*, S−S*, S−M*, M−M−SG1, M−S−SG1, S−S−SG1, and S−M−SG1, where SG1 is the nitroxyl radical. During the reaction, a living chain can thus be switched to a different category when its ultimate unit or living status is changed, as shown in Figure 2. When a chain is terminated by termination or chain transfer, it is categorized as a dead polymer. Kinetic parameters for all of the reactions included in the mechanism are reported in Table 1.

Table 1. Kinetic Parameters use in MMA/S KMC Simulations

reactions	frequency factors, A (s^{-1}, L mol^{-1} s^{-1} or L^2 mol^{-2} s^{-1})	activation engergy, E_a (kcal/mol)
initiator dissociation[28]	2.4×10^{14}	26.84
initiator radical addition to S monomer[30 a]	3.16×10^{7}	2.44
initiator radical addition to MMA monomer[30 a]	1.0×10^{9}	0.62
thermal initiation of S monomer[31]	6.3×10^{5}	27.44
homopropagation of MMA-terminated radical chains[32 b]	2.67×10^{7}	5.35
homopropagation of S-terminated radical chains[33 b]	4.27×10^{7}	7.76
disproportionation between MMA-terminated radical chains[35,36 c,d]	8.16×10^{8}	2.84
combination between MMA-terminated radical chains[35,36 c,d]	5.44×10^{8}	2.84
disproportionation between S-terminated radical chains[37 d]	4.31×10^{8}	1.5
combination between S-terminated radical chains[37 d]	2.45×10^{9}	1.5
chain transfer to MMA monomer[38 e]	2.67×10^{2}	5.35
chain transfer to S monomer[39]	2.31×10^{6}	12.67
decoupling of M−M−SG1[40]	2.4×10^{14}	24.86
decoupling of S−M−SG1[40]	2.4×10^{14}	25.81
decoupling of M−S−SG1[40]	2.4×10^{14}	27.49
decoupling of S−S−SG1[40]	2.4×10^{14}	29.88

reactions	rate coefficient (L mol^{-1} s^{-1})
coupling of initiator[29 f]	2.0×10^{6}
coupling of MMA-terminated radical chains[27 g]	4.0×10^{4}
coupling of S-terminated radical chains[41 f]	4.75×10^{5}

[a] The addition rate constants of initiator radical to S and MMA monomers were determined by the experimental data of the primary radical $(CH_3)_2\dot{C}OH$ with S and MMA monomers. [b] Penultimate reactivity ratios were obtained from the work of Fukuda et al. as $r_{11} = r_{21} = 0.523$, $r_{22} = r_{12} = 0.46$, $s_1 = 0.3$, $s_2 = 0.53$, in which monomer 1 is S and monomer 2 is MMA.[34] [c] Determined by the disproportionation/combination ratio k_{td}/k_{tc} of MMA-terminated radical chains.[36] [d] The rate constants of cross-termination reactions between MMA-terminated radical chains and S-terminated radical chains were determined as the geometric mean of the homotermination reaction rate coefficients. [e] Determined by k_{tr}/k_p value.[38 f] Determined by extrapolation from the experimental data. [g] Weakly dependent on temperature, so an average value over the temperature range of 10−50 °C was used.

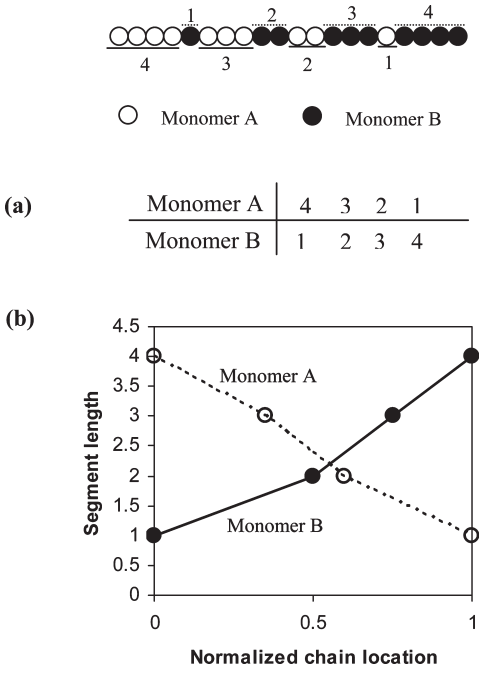

Figure 3. (a) Data structure used in the KMC framework to record the explicit sequence of each copolymer chain. (b) Variation of segment lengths along a chain which is transformed from the explicit sequence of the chain predicted by the KMC framework.

As shown in Figure 3a, the explicit sequence of each chain is tracked by recording the length of each individual segment, which is the number of repeating units comprising the segment, in sequence from the initiation of the chain (denoted as the "head of the chain" in this work) to the end of reaction or the termination of the chain (denoted as the "tail of the chain" in this work). A new segment is generated when a cross-propagation reaction occurs, and the length of a segment is increased by one when a homopropagation reaction occurs. If a living chain is terminated by disproportionation or chain transfer, the sequence of the chain is known exactly and fixed. The sequence of a dead polymer chain terminated by combination, in which two radical chains are combined tail to tail, is determined by connecting the sequence of one radical chain with the "reversed" sequence of the other radical chain. Here, the reversed sequence of a chain is denoted as the sequence from the tail to the head of the chain.

Scaling of the KMC Model. In all the simulations reported in this work, 10^9 monomers were initially put into the reactor in the beginning of the reaction, which can generate around 1.3×10^6 individual chains in the system with the initiator concentration used in this work. As the reaction proceeds, the total amount of monomer is further increased because of the addition of the second monomer to the system. An initial number of monomers of 10^9 was determined to be a sufficiently large sample size based on the fact that the simulation results were in very close agreement with those from simulations using 10^{10} monomers initially.

Characterization of Chain Sequence. KMC simulations can predict the explicit sequence of each chain, which allows for analysis of the entire population of copolymer chains at various levels of detail. It is possible not only to extract the average properties of the copolymer system, such as number-average and weight-average molecular weight and average copolymer composition, but also to perform the more detailed analysis related to properties of each individual chain, such as the chemical composition distribution, in a facile way.

However, there is no existing method to extract measures of chain sequence from the voluminous data that describe the characteristics of the entire population of chains in a concise yet comprehensive way. Here, we propose a quantitative approach to map out the average trend of variation of segment lengths along copolymer chains in the entire population as follows. First of all, the normalized chain location, which denotes the relative location of the segment on the chain, is assigned to each segment according to the following rules. The locations of the first segments of each type of

monomer that were formed after the initiation of the chain were fixed at a normalized chain location of 0, and the last segments of each type of monomer were fixed at a normalized chain location of 1. The location of a segment in between was determined by the ratio of the distance from the head of the chain to the last monomer comprising the segment over the total length of the chain. In this way, the sequence information on each individual chain can be depicted as a series of dots on a scatter plot, where the *y*-coordinate corresponds to the length of the segment and the *x*-coordinate corresponds to the relative location of the segment on the normalized chain length. Finally, these discrete dots representing the sequence information on a chain were transformed into a continuous trend line by connecting any neighboring segments of the same monomer type by a straight line as shown in Figure 3b. In this way, the sequence of each individual chain can be represented quantitatively within the same axial scale, which allows for further statistical analysis for the whole population of chains.

In order to capture the average trend of the variation of the segment lengths along copolymer chains in the whole population, we predicted the number-average and weight-average segment lengths, N_n and N_w, at each normalized chain location. The number-average and the weight-average segment lengths of monomer j at location i in a system of m chains, $Nn_{j,i}$ and $Nw_{j,i}$, was calculated as follows:

$$Nn_{j,i} = \frac{\sum_{p=1}^{m} Nn_{j,i,p}}{m} \tag{4}$$

$$Nw_{j,i} = \sum_{p=1}^{m} \frac{Nn^2_{j,i,p}}{\sum_{p=1}^{m} Nn_{j,i,p}} \tag{5}$$

The average variation of the segment lengths along the chain in the whole population can be represented by N_n as a function of its normalized chain location. In addition, the polydispersity of the segment lengths formed at the same normalized location of different chains was characterized by the polydispersity index of local segment lengths (segment PDI) which is the ratio of the weight-average segment length over the number-average segment length at that location, $Nw_{j,i}/Nn_{j,i}$. Similar to the concept of the molecular weight PDI, M_w/M_n, the local segment PDI approaches unity as the distribution of the segment lengths formed at the same location is narrow. The reproducibility of the whole sequence from chain to chain can be thus be evaluated by the local segment PDI along the chain.

Experimental Section

Gradient Copolymer Synthesis. Styrene (S) (99%, Aldrich) and methyl methacrylate (MMA) (99%, Aldrich) monomers were deinhibited by combining with *tert*-butylcatechol remover (Aldrich) and monomethyl ether hydroquinone remover (Aldrich), respectively, as well as calcium hydride and stirring for at least 8 h at room temperature in the dark. Two different syntheses were carried out, which differed by which monomers were fed and initially charged to the reactor. To differentiate them, we adopted the naming convention P-(monomer A-*grad*-monomer B), where monomer A is the type of monomer fed into the system, while monomer B is the type of monomer initially predominant in the reactor charge at the beginning of the reaction. P(S-*grad*-MMA) and P(MMA-*grad*-S) were synthesized in a semibatch mode using NM-CRP with *N*-(2-methylpropyl)-*N*-(1-diethylphosphono-2,2-dimethylpropyl)-*O*-(2-carboxyl-prop-2-yl)hydroxylamine, or MAMA-SG1 (BlocBuilder), as the nitroxide initiator. P(S-*grad*-MMA) was prepared by adding S at 2.5 mL/h continuously through the entire reaction into an MMA-rich environment (4 mL of MMA, 1 mL of S, and 20 mg of initiator in a 25 mL round-bottomed flask at the beginning of the reaction) and reacting at 368 K for 6 h. P(MMA-*grad*-S) was prepared by adding MMA at 2.5 mL/h continuously through the entire reaction into S (5 mL of S and 20 mg of initiator in a 25 mL round-bottomed flask as the initial charge) and reacting at 368 K for 8 h. Approximately 1 mL aliquots were taken periodically during the reaction for characterization purposes. The aliquots and final products were precipitated in cold methanol and then dried at 70 °C under vacuum overnight.

Characterization. The molecular weights and polydispersities of the aliquots and the final products were determined by gel permeation chromatography (GPC) using universal calibration with PS standards. For both copolymers, the molecular weights increased and polydispersities decreased as a function of reaction time. For P(MMA-*grad*-S), M_n ranged between 11 000 and 147 000 g mol^{-1}, and the PDI varied between 1.9 and 1.5. For P(S-*grad*-MMA), M_n ranged between 6700 and 31 000 g mol^{-1}, and the PDI varied between 1.5 and 1.3. F_S and F_{MMA} were analyzed by ^{1}H NMR (Varian, 500 MHz) in $CDCl_3$ solution at 1 mg mL^{-1} in 5 mm diameter probes. The integral values from the aromatic protons on the styrene repeat units (6.2−7.2 ppm) and all other protons associated with lower chemical shift values (0.6−4.5 ppm) were compared to calculate F_S. Monomer conversion values were low and subject to large fluctuations, so they are not reported here.

The triad distribution was analyzed by ^{13}C NMR (Avance III, Bruker, 500 MHz) in $CDCl_3$ solution at 100 mg mL^{-1} in 5 mm diameter probes. All the data were collected with 512 scans. $F_{MMM}/(F_{MMM} + F_{MMS})$ was calculated by comparing the integral values from the peaks C (17.1−19.2 ppm) and D (15.8−17.1 ppm) of the α-methyl carbon of MMA repeat units.[42]

Results and Discussion

Validation of KMC Simulations. The populations of copolymer chains generated from the two different synthesis conditions were simulated by the KMC framework. In order to mimic the actual experimental conditions, the reaction volume and numbers of species were updated to account for the addition of monomers and removal of samples for characterization purposes.

Figure 4 summarizes the characterization features of two synthesized gradient copolymers and compares the simulated results against experimental data. The styrene cumulative composition F_S of P(MMA-*grad*-S) decreases with increasing reaction time from a value of 1 at the beginning of the reaction to 0.24 at the end of the reaction. Compared to P(MMA-*grad*-S), the variation of F_s in P(S-*grad*-MMA) is milder, increasing from 0.37 at 1 h of the reaction to 0.52 at the end of the reaction. Note that F_S does not start from zero for P(MMA-*grad*-S) because it is necessary to add some amount of styrene into the initial batch to maintain the MMA-rich system as living. Molecular weight values also increased as a function of reaction time. Therefore, the copolymer composition as a function of chain length varied monotonically in both syntheses, which is typically considered as a unique characteristic of gradient copolymers.[6,10,16,17] As shown in Figure 4a,b, the simulations match the evolution of F_S very well.

Comparison of the predicted and measured triad distributions provided a more stringent test of the KMC simulations. Triad distributions were measured which is the most direct

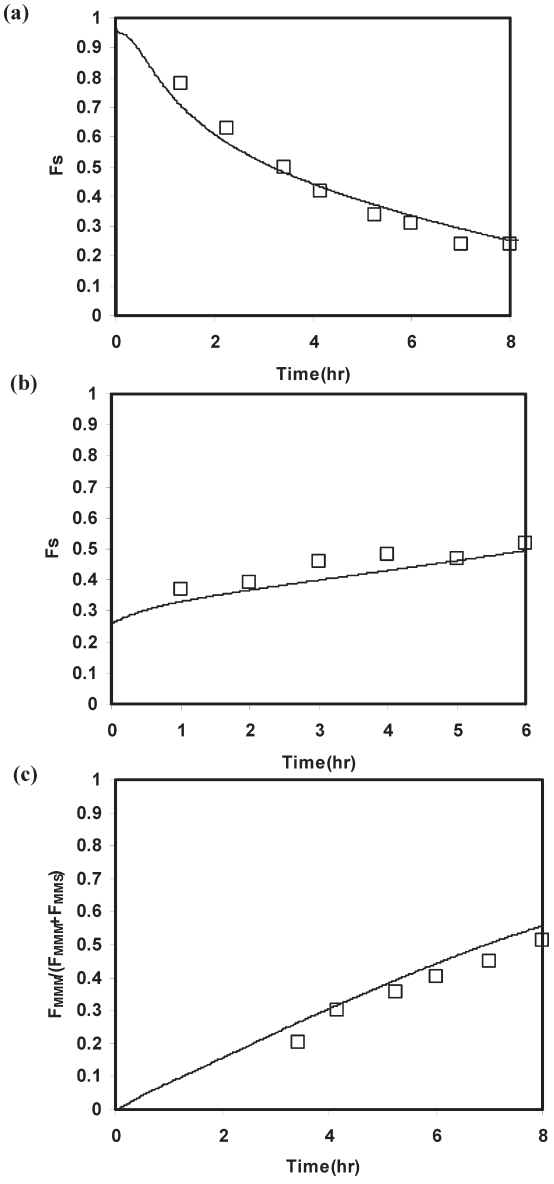

Figure 4. Experimental characterization (open squares) and predictions generated from KMC simulations (solid lines) of synthesized gradient copolymers: (a) evolution of cumulative styrene mole fraction, F_S, of P(MMA-*grad*-S) as a function of reaction time; (b) evolution of F_S of P(S-*grad*-MMA) as a function of reaction time; (c) evolution of the fraction of MMA-centered triad MMM over the sum of MMM and MMS triads, $F_{MMA}/(F_{MMM} + F_{MMS})$, of P(MMA-*grad*-S) as a function of reaction time.

information related to sequence among the experimental measures that are available. As shown in Figure 4c, the ratio of MMA-centered triads, MMM, to the sum of the MMM and MMS triads, $F_{MMM}/(F_{MMM} + F_{MMS})$, of P(MMA-*grad*-S) is predicted by the simulations very well. This ratio increases from 0.2 at 3.5 h of reaction to 0.5 at the end of the reaction, which reveals that there is an increasing proportion of MMA homopolymer segments as chain length increases. It is important to note, however, that the simulations can even predict the monomer-by-monomer sequence along each copolymer chain, which is not yet accessible experimentally.

Monomer-by-Monomer Sequence along Copolymer Chains. Since the introduction of gradient copolymers, the microstructure formed along copolymer chains has been characterized by the compositional gradient, which is the variation of the local copolymer composition along the

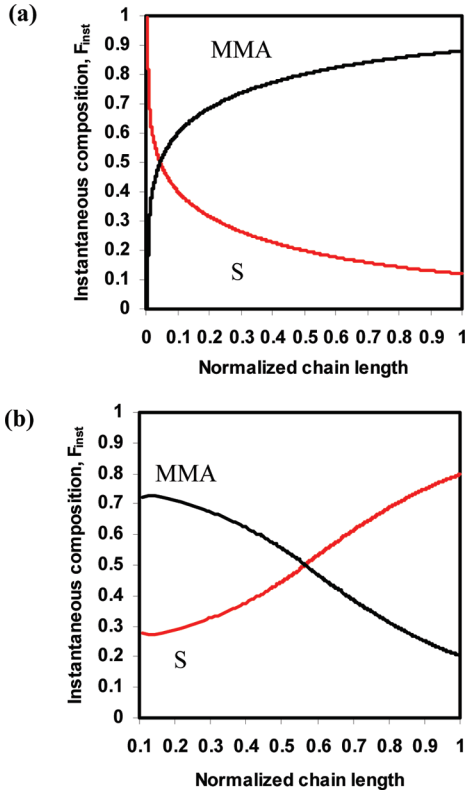

Figure 5. Instantaneous composition as a function of normalized chain length: (a) P(MMA-*grad*-S); (b) P(S-*grad*-MMA).

chain, in the majority of theoretical research related to gradient copolymers. For gradient copolymers synthesized with LRP, the compositional gradient is typically represented by F_{inst} as a function of chain length. Thus, for comparison purposes, the evolution of F_{inst} for the two different systems was predicted first. As shown in Figure 5, the instantaneous compositions are smooth functions as normalized chain length increases and vary as expected for both systems. P(MMA-*grad*-S) has an S-rich head with $F_{inst,s}$ close to 1 at the head of the chains and an MMA-rich tail with $F_{inst,MMA}$ around 0.9 at the end of the chains. Because of the different feed order than that used to synthesize P(MMA-*grad*-S), P(S-*grad*-MMA) has an MMA-rich head with $F_{inst,MMA}$ equal to 0.7 at the head of the chains and an S-rich tail with $F_{inst,S}$ close to 0.8 at the end of the chains. Thus, both gradient copolymers have strong compositional gradients along the chains.

The variation of Nn_{MMA} and Nn_S as a function of normalized chain location of both systems was predicted and is shown in Figure 6. There are two particularly striking features of the predicted monomer-by-monomer sequences. First, the simulation results show that the number-average segment lengths formed in both copolymers are surprisingly short even when the chain composition heavily favors one monomer and the overall chain length is high. For example, for P(S-*grad*-MMA) chains, the average S segment length at the tail accounts for less than 0.3% of the total chain length and never exceeds a value of four, even when the instantaneous composition is as high as 0.8. For P(MMA-*grad*-S), the average segment length of S is reasonably high at the head of the chains, but it plummets very quickly and achieves a constant value of around two for the large majority (~80%) of the chain interior at the end of the batch. These number-average sequence lengths present a stark contrast to the sequences expected based on average composition measures.

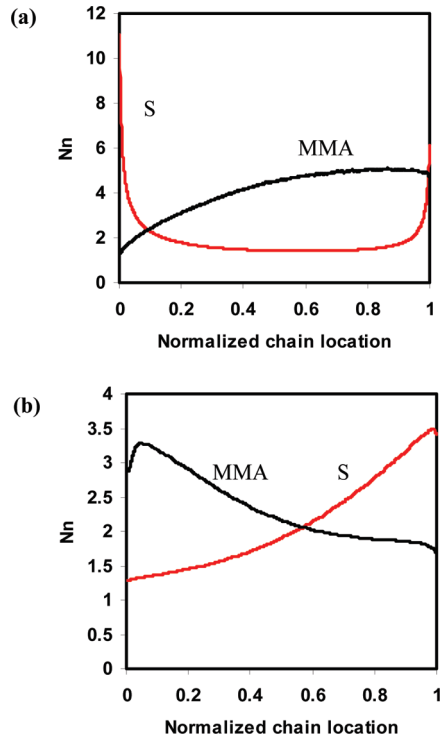

Figure 6. Number-average segment length, N_n, as a function of normalized chain location of (a) P(MMA-*grad*-S) and (b) P(S-*grad*-MMA).

Scheme 1. Schematic Representation of the Composition in Block, Gradient and Random Copolymers, in which the Open Circles Denote Monomer A and the Closed Circles Denote Monomer B

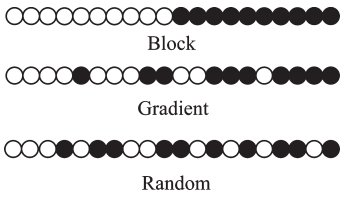

The explicit monomer sequence of the final products of both copolymers resembles that of a random copolymer more closely than it does the ideal sequence of a gradient copolymer depicted in Scheme 1.

The second striking feature of the segment length maps in Figure 6 is manifested in the S segment lengths of P(MMA-*grad*-S). There is a clear upward bend at the tail, although F_S decreases continuously during the reaction. Thus, the condition defining a gradient copolymer based on F or F_{inst} is met, but the monomer-by-monomer sequence is in fact dramatically different than what is expected for a gradient copolymer. The results of the KMC simulations reveal the origin of this behavior. Since MMA cannot be controlled in NM-CRP, the livingness of the reaction decreases as the amount of MMA monomer in the reaction system increases. In the later stage of the synthesis, dead polymer chains account for over 60% of the total chains existing in the system. The dead chains are formed primarily by recombination (> 70%), despite the MMA-rich environment. Styrene-terminated chains are the most abundant living chains, and thus, termination is chiefly governed by styrene. Thus, there are a large number of chains that essentially have a sequence axis of symmetry, leading to chains that are styrene-rich at both ends and differ substantially from the desired gradient microstructure.

Our findings indicate that even a very large change in instantaneous composition can correspond to a minor change

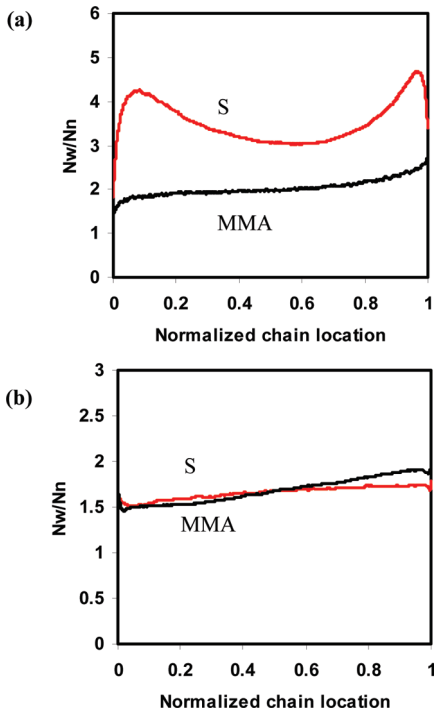

Figure 7. Local segment PDI of S and MMA segments as a function of normalized chain location of (a) P(MMA-*grad*-S) and (b) P(S-*grad*-MMA).

in N_n. For example, as shown in Figure 5b, $F_{inst,MMA}$ of P(S-*grad*-MMA) decreases from 0.7 at the early stage to 0.2 at the final stage of the polymerization, while N_n of MMA segments varies by less than two units long. While this effect has been observed here for MMA/S copolymers, other copolymer systems where the reactivity ratios are all less than 1 can exhibit the same behavior. In addition, the observation that the overall shape of the number-average segment length along the chain can significantly deviate from that of the instantaneous composition as a function of chain length when combination is the favored termination mode is also generalizable. Overall, the details of explicit sequence along the chain that are revealed by the KMC simulations are obscured by only considering fractional composition measures, F or F_{inst}, to characterize the gradient shape.

Uniformity of Sequence Pattern along Copolymer Chains. Typically, a synthesized copolymer system is not monodisperse, but instead copolymers of different chain lengths, sequences, and compositions coexist. Thus, fluctuations around the average properties, such as molecular weight PDI, are also of utter importance in characterizing a polymer system. The overall picture of the sequences formed in the two systems has been provided above in the form of the variation of number-average segment lengths as a function of normalized chain location. Here, we further investigated the uniformity of sequence patterns formed on different copolymer chains in the whole population by predicting the local segment PDI as a function of normalized chain location. Figure 7 shows the local segment PDI of S and MMA as a function of normalized chain location for the two gradient copolymer systems.

On the basis of these plots, the uniformity of the sequence pattern in P(S-*grad*-MMA) is superior to that in P(MMA-*grad*-S). The local segment PDI values of S and MMA in P(S-*grad*-MMA) increase slightly toward the end of the chains, but they are both lower than two throughout the chain length. In P(S-*grad*-MMA), the local segment PDI of S is

extremely high, exceeding a value of three throughout the chain, and has two maxima, one near each end of the chain. In forced gradient copolymerization, monomer composition changes continuously during the reaction, but only a small portion of living chains may be reactivated to propagating radicals at a given monomer composition. As shown in Figure 5, $F_{inst,S}$ in P(MMA-*grad*-S) plummeted quickly from around 1 to below 0.5 in the early stage of the reaction. Thus, long segments of S were formed at the head of the dormant chains activated in the very early stage of the reaction when S monomer was strongly favored, while much shorter segments of S were formed at the similar chain location in the dormant chains which were activated in a later stage of the reaction. Thus, a broad distribution of segment lengths of S was formed near the head of chains in P(MMA-*grad*-S) which is manifested by a peak in the local segment PDI near the head. In addition, in the population of P(MMA-*grad*-S), there is an amount of dead polymers with a symmetric monomer sequence resulting from the tail-to-tail combination of two radicals, which can significantly increase the segment PDI near the tail of chains.

The molecular weight PDI is widely used as a criterion to characterize the uniformity of chain growth. If the molecular weight PDI is under 1.5, the polymer system is typically viewed as narrowly distributed. The molecular weight PDI of P(MMA-*grad*-S) is 1.5, which indicates a relatively narrow distribution of molecular masses. However, KMC simulations reveal that P(MMA-*grad*-S) actually has a broad distribution of sequence patterns along the chain in the whole population. Our finding suggests that local sequence can be quite disperse even if the macromolecular masses are relatively uniform. The uniformity of monomer sequence among different chains can be affected by the details in chain growth history which may have only trivial impacts on molecular weight PDI. Thus, it is possible to overestimate the uniformity of a sequence pattern along the chain by only considering the value of molecular weight PDI.

High uniformity of sequence patterns would be preferred in the investigation of the relationship between the physical properties of gradient copolymers and the sequence along the chain, but the local segment PDI can be affected by many factors during the reaction. The reaction conditions need to be carefully tuned throughout the reaction in order to achieve high reproducibility of sequences in the whole population. Since reproducibility of sequences cannot be investigated by current experimental techniques, it is necessary to utilize computer simulations in optimizing synthesis recipes in order to achieve a narrow distribution of sequence patterns along the chain in the entire population.

Structural Gradient Copolymers. On the basis of our findings, large changes in local copolymer composition may correspond to only trivial changes in segment lengths. Gradient copolymers with a compositional gradient along the chain do not necessarily have a corresponding variation in the segment lengths. However, the variation of the segment lengths and the alignments of these segments along the copolymer chain play a very important role in some applications involving gradient copolymers, such as interfacial activities. Thus, we propose that it is necessary to further stratify what is characterized as a gradient copolymer.

Here, we categorize gradient copolymers into two distinct classes: "compositional" gradient copolymers, which have a continuous change in chemical composition along the copolymer chains, and "structural" gradient copolymers, whose sequence lengths change according to a particular pattern from one end to the other. Structural gradient copolymers also have a compositional gradient along the chain, but compositional gradient copolymers do not necessarily have an obvious structural gradient along the chain. While the relationship between the compositional gradient along the chain and physical properties of gradient copolymers has been studied intensely in the past decade,[43−48] the impact of the variation of segment lengths along the copolymer chain on the physical properties of gradient copolymers is still elusive. In order to unravel these relationships, there must be a shift from a focus on control of composition to control of sequence.

Conclusions

A simulation framework based on kinetic Monte Carlo, which can predict the explicit sequence formed along each chain by tracking the growth of each individual chain, was reported. The framework is generally applicable to various reaction types and can incorporate differences in reactivity of different chain ends in a facile way. The copolymerization of MMA/S gradient copolymers prepared by NM-CRP was simulated using this KMC framework as an example. In order to validate the KMC model, two S/MMA gradient copolymers, P(S-*grad*-MMA) and P(MMA-*grad*-S), were synthesized by forced gradient copolymerization with BlocBuilder as the initiator and characterized experimentally. The KMC model was able to capture the experimental data very well. The explicit sequences along the backbones of P(S-*grad*-MMA) and P(MMA-*grad*-S) were then predicted. It was found that the number-average segment lengths formed in both copolymers are surprisingly short even when the local copolymer composition heavily favors one monomer. In addition, it was found that the overall shape of the number-average segment length along the chain can significantly deviate from that of the instantaneous composition as a function of chain length when combination is the favored termination mode. These details of explicit sequence along the chain revealed by KMC simulations are obscured by only considering fractional composition measures to characterize the gradient shape. The uniformity of sequence patterns formed on different copolymer chains in these two gradient copolymer systems was also investigated. It was found that local sequence can be quite disperse even if the molecular weight PDI of the entire population is low. In order to achieve a high degree of uniformity of sequences along the chain, the reaction conditions need to be carefully tuned throughout the reaction. On the basis of these findings, we proposed to further categorize gradient copolymers into compositional gradient copolymers as well as structural gradient copolymers.

We have shown here that KMC simulations are a powerful tool to predict the explicit sequence of copolymers and can serve as a companion to experimental efforts to precisely design the sequence length along copolymer chains. Current efforts to utilize KMC simulations to develop synthesis recipes to meet design targets of sequence patterns along copolymer chains are underway.

Acknowledgment. This work was supported by the MRSEC program of the National Science Foundation (DMR-0520513) at the Materials Research Center of Northwestern University.

References and Notes

(1) Beginn, U. *Colloid Polym. Sci.* **2008**, *286*, 1465–1474.
(2) Matyjaszewski, K.; Ziegler, M. J.; Arehart, S. V.; Greszta, D.; Pakula, T. *J. Phys. Org. Chem.* **2000**, *13*, 775–786.
(3) Jakubowski, W.; Juhari, A.; Best, A.; Koynov, K.; Pakula, T.; Matyjaszewski, K. *Polymer* **2008**, *49*, 1567–1578.
(4) Shull, K. R. *Macromolecules* **2002**, *35*, 8631–8639.
(5) Kim, J.; Zhou, H.; Nguyen, S. T.; Torkelson, J. M. *Polymer* **2006**, *47*, 5799–5809.

(6) Kim, J.; Mok, M. M.; Sandoval, R. W.; Woo, D. J.; Torkelson, J. M. *Macromolecules* **2006**, *39*, 6152–6160.
(7) Lefebvre, M. D.; de la Cruz, M. O.; Shull, K. R. *Macromolecules* **2004**, *37*, 1118–1123.
(8) Mok, M. M.; Pujari, S.; Burghardt, W. R.; Dettmer, C. M.; Nguyen, S. T.; Elllison, C. J.; Torkelson, J. M. *Macromolecules* **2008**, *41*, 5818–5829.
(9) Goto, A.; Fukuda, T. *Prog. Polym. Sci.* **2004**, *29*, 329–385.
(10) Dettmer, C. M.; Gray, M. K.; Torkelson, J. M.; Nguyen, S. T. *Macromolecules* **2004**, *37* (15), 5504–5512.
(11) Berezkin, A. V.; Khalatur, P. G.; Khokhlov, A. R. *Macromolecules* **2006**, *39*, 8808–8815.
(12) Gorman, C. B.; Petrie, R. J.; Genzer, J. *Macromolecules* **2008**, *41*, 4856–4865.
(13) Park, J. S.; Kataoka, K. *Macromolecules* **2006**, *39*, 6622–6630.
(14) Lee, H.; Matyjaszewski, K.; Yu, S.; Sheiko, S. S. *Macromolecules* **2005**, *38* (20), 8264–8271.
(15) Mignard, E.; Lablanc, T.; Bertin, D.; Guerret, O.; Reed, W. F. *Macromolecules* **2004**, *37*, 966–975.
(16) Min, K.; Li, M.; Matyjaszewski, K. *J. Polym. Sci., Part A: Polym. Chem.* **2005**, *43*, 3616–3622.
(17) Min, K.; Oh, J. K.; Matyjaszewski, K. *J. Polym. Sci., Part A: Polym. Chem.* **2007**, *45*, 1413–1423.
(18) Zargar, A.; Schork, F. J. *Macromol. React. Eng.* **2009**, *3*, 10.1002 (DOI).
(19) Beginn, U. *Polymer* **2006**, *47*, 6880–6894.
(20) Wang, R.; Luo, Y.; Li, B.; Sun, X.; Zhu, S. *Macromol. Theory Simul.* **2006**, *15*, 356–368.
(21) Sun, X.; Luo, Y.; Wang, R.; Li, B.; Liu, B.; Zhu, S. *Macromolecules* **2007**, *40*, 849–859.
(22) Dotson, N. A.; Galvan, R.; Laurence, R. L.; Tirrell, M. *Polymerization Process Modeling*; VCH Publishers Inc.: New York, 1995.
(23) Khalatur, P. G.; Khokhlov, A. R. *Adv. Polym. Sci.* **2006**, *195*, 1–100.
(24) Starovoitova, N. Y.; Berezkin, A. V.; Kriksin, Y. A.; Gallyamova, O. V.; Khalatur, P. G.; Khokhlov, A. R. *Macromolecules* **2005**, *38*, 2419–2430.
(25) Tabash, R. Y.; Teymour, F. A.; Debling, J. A. *Macromolecules* **2006**, *39*, 829–843.
(26) Gillespie, D. T. *J. Comput. Sci.* **1976**, *22*, 403–434.
(27) Guillaneuf, Y.; Gigmes, D.; Marque, S. R. A.; Tordo, P.; Bertin, D. *Macromol. Chem. Phys.* **2006**, *207*, 1278–1288.
(28) Bertin, D.; Gigmes, D.; Marque, S. R. A.; Tordo, P. *Macromolecules* **2005**, *38*, 2638–2650.
(29) Sobek, J.; Martschke, R.; Fischer, H. *J. Am. Chem. Soc.* **2001**, *123*, 2849–2857.
(30) Fischer, H.; Radom, L. *Angew. Chem., Int. Ed.* **2001**, *40*, 1340–1371.
(31) Campbell, J. D.; Teymour, F.; Morbidelli, M. *Macromolecules* **2003**, *36*, 5491–5501.
(32) Beuermann, S.; Buback, M.; Davis, T. P.; Gilbert, R. G.; Hutchinson, R. A.; Olaj, O. F.; Russell, G. T.; Schweer, J.; Van Herk, A. M. *Macromol. Chem. Phys.* **1997**, *198*, 1545–1560.
(33) Buback, M.; Kuchta, F. D. *Macromol. Chem. Phys.* **1997**, *198*, 1455–1480.
(34) Fukuda, T.; Ma, Y. D.; Inagaki, H. *Macromolecules* **1984**, *18*, 17–26.
(35) Brandrup, J.; Immergut, E. H.; Grulke, E. A. *Polymer Handbook*, 4th ed.; Wiley: New York, 1999.
(36) Moad, G.; Solomon, D. H. *The Chemistry of Free Radical Polymerization*; Elsevier Science: New York, 1995.
(37) Cho, A. S. Mechanistic Modeling of Nitroxide-Mediated Controlled Radical Polymerization. Ph.D. Thesis, Northwestern University, **2009**.
(38) Meyer, T.; Keurentjes, J. *Handbook of Polymer Reaction Engineering*; Wiley-VCH, Verlag GmbH & Co.: Weinheim, 2005.
(39) Hui, A. W.; Hamielec, A. E. *J. Appl. Polym. Sci.* **1972**, *16*, 749–769.
(40) Nicolas, J.; Dire, C.; Mueller, L.; Belleney, J.; Charleux, B.; Marque, S. R. A.; Bertin, D.; Magnet, S.; Couvreur, L. *Macromolecules* **2006**, *39*, 8274–8282.
(41) Guillaneuf, Y.; Bertin, D.; Castigolles, P.; Charleux, B. *Macromolecules* **2005**, *38*, 4638–4646.
(42) Aerdts, A. M.; de Haan, J. W.; German, A. L. *Macromolecules* **1993**, *26*, 1965–1971.
(43) Pickett, G. T. *J. Chem. Phys.* **2003**, *118*, 3898.
(44) Aksimentiev, A.; Holyst, R. *J. Chem. Phys.* **1999**, *111*, 2329.
(45) Karaky, K.; Pere, E.; Pouchan, C.; Desbrieres, J.; Derail, C.; Billon, L. *Soft Matter* **2006**, *2*, 770–778.
(46) Jiang, R.; Jin, Q.; Li, B.; Ding, D. *Macromolecules* **2008**, *41*, 5457–5465.
(47) Wang, R.; Li, W.; Luo, Y.; Li, B.; Shi, A.; Zhu, S. *Macromolecules* **2009**, *42*, 2275–2285.
(48) Kim, J.; Gray, M. K.; Zhou, H.; Nguyen, S. T.; Torkelson, J. M. *Macromolecules* **2005**, *38*, 1037–1040.